Biology of Reproduction, 2017, 97(4), 644–655
doi:10.1093/biolre/iox106
Research Article
Advance Access Publication Date: 28 August 2017

Research Article

Stage-specific follicular extracellular vesicle uptake and regulation of bovine granulosa cell proliferation†

Wei-Ting Hung[1], Raphatphorn Navakanitworakul[1,2], Tarique Khan[3], Pan Zhang[4], John S. Davis[4], Lynda K. McGinnis[5] and Lane K. Christenson[1,*]

[1]Department Molecular and Integrative Physiology, University of Kansas Medical Center, Kansas City, Kansas, USA; [2]Department of Biomedical Sciences, Faculty of Medicine, Prince of Songkla University, Hatyai, Songkhla, Thailand; [3]Stowers Institute for Medical Research, Kansas City, Missouri, USA; [4]Department of Obstetrics and Gynecology, University of Nebraska Medical Center and VA Nebraska-Western Iowa Health Care System, Omaha, Nebraska, USA and [5]Department Obstetrics and Gynecology, University of Southern California, Norris Cancer Center, Los Angeles, California, USA

*__Correspondence:__ Department of Molecular and Integrative Physiology, University of Kansas Medical Center, 3901 Rainbow Blvd., Mail Stop 3043, Kansas City, KS 66160, USA. Tel: +913-588-0420; Fax: +913-588-7180; Email: lchristenson@kumc.edu

†__Grant Support:__ We also wish to acknowledge several core facilities that were essential for completion of this work: University of Kansas Medical Center Electron Microscopy Research Lab facility is supported in part, by NIH COBRE grant 9P20GM104936. The JEOL JEM-1400 TEM used in the study was purchased with funds from NIH grant S10RR027564.The work was funded by National Institute of Child Health and Human Development: HD061580 to LKC and HD082484 to LKC and LKM, Olson Center for Women's Health and Department of Veterans Affairs Office of Research and Development Biomedical Laboratory Research and Development funds to JSD.

Received 28 February 2017; Revised 30 June 2017; Accepted 25 August 2017

Abstract

Follicular fluid within ovarian antral follicles contains numerous factors, which influence the development of a healthy oocyte including nucleic acids, steroids, proteins, and extracellular vesicles (EVs). Current evidence indicates that follicular EVs promote changes in cellular gene expression and support cumulus–oocyte complex expansion in vitro. In this study, we found EVs from different sized follicles differentially stimulate granulosa cell proliferation and this could be explained by both the differential contents associated, on or within the vesicles and by the preferential uptake of EVs dependent on follicle size from which they were isolated. Antibody array and inhibitor studies indicated that the Src, PI3K/Akt, and MAPK signaling pathways mediate the stimulatory effects of EVs on granulosa cell proliferation. This study demonstrates for the first time that EVs isolated from follicular fluid are capable of stimulating granulosa cell proliferation and that this stimulatory response is associated with the size of antral follicle from which the EVs originated. The study further also provides the first evidence that vesicles released by small antral follicles are preferentially taken up when compared to those isolated from large follicles, suggesting that vesicular surface proteins change during follicular maturation.

Summary Sentence

Follicular fluid derived extracellular vesicles exhibit differential ability to stimulate granulosa cell proliferation and uptake that is dependent upon the stage of follicle development.

Key words: extracellular vesicles, exosomes, follicular fluid, follicle, granulosa cell, proliferation, Src, MAPK, and PI3K.

Introduction

During the later stages of folliculogenesis, the follicle is defined by the formation of an antrum, which is filled with a serum-like exudate called follicular fluid (FF) [1]. The antral cavity containing FF isolates the oocyte and its associated cumulus cells from the endocrine mural granulosa cells (GCs), thus presumably providing a hospitable environment for the normal development of a fertile oocyte. This isolation, however, has given rise to intricate paracrine/juxacrine networks that facilitate the exchange of cellular messages between the cumulus-enclosed oocyte and the segregated mural GCs [2]. Recently, in addition to numerous proteins, steroids, lipids, and nucleic acids, extracellular vesicles (EVs) have been found in the FF, and they have been hypothesized to act as yet another cellular mechanism to facilitate cross talk across the follicular antrum [3–7].

Release of EVs appears to be a phenomenon exhibited by all cells with two major known mechanisms of EV biogenesis [8]. The first includes exosome biogenesis, where inward budding of the multivesicular body (MVB) membrane generates intraluminal vesicles (i.e. exosomes of 30–200 nm diameter) that are released into the extracellular space upon fusion of the MVB with the plasma membrane [9]. The second includes microvesicles that are produced by plasma membrane blebbing and results in a broad range (30–1000 nm) of vesicles sizes [10]. Due to the overlap of markers and sizes of exosomes and microvesicles, EVs has been adopted as an inclusive term that encompasses both kinds of vesicles outside the plasma membrane [11].

Currently, EVs isolated from FF have been shown to carry different microRNA (miRNA) dependent upon the origin of the samples; e.g. stages of follicular maturation, age, and disease conditions such as polycystic ovarian syndrome [3–7, 12–14]. In addition, ovarian GCs isolated from multiple species have been shown to take up fluorescently labeled vesicles [3–7, 12–14]. Determination of whether FF EVs actually might have a function within the follicle however is very limited. Gene expression analysis of mare GCs treated with follicular EVs from both mid-estrous and pre-ovulatory follicles showed decreased expression of inhibitor of DNA binding/differentiation 2 (*ID2*), a target of abundant miRNAs found within FF EVs [15]. Treatment of cumulus–oocyte complexes with EVs isolated from FF induced cumulus expansion and initiated the corresponding gene expression changes associated with cumulus expansion in bovine and mice [16]. Both of these studies while indicating a "functional effect" of EVs are however compromised by the purity of EV preparations, as EV isolation even under "gold-standard" ultracentrifugation protocols is far from 100% pure. This has raised concerns of whether material that co-purifies may also contribute to the functional effects attributed to EVs. In our original study of cumulus cell expansion [16], we observed different functional effects (i.e. gene expression differences) of follicular EVs based on the size of the follicle from which the EVs were isolated. In the current study, we investigate whether mural GCs, the predominant cell type within the antral follicle, exhibit a functional response (i.e. cell proliferative and EV uptake) following exposure to stage-specific follicular EVs. We applied a combination of EV isolation methodologies to yield highly purified EVs and then examined their effects on cell signaling pathways involved in cellular proliferation and EV uptake by cultured GCs.

Materials and methods

Follicular fluid collection

Bovine ovaries were collected from a local abattoir and because the animals were not used specifically for research purposes our Institutional Animal Care and Use Committee ruled that the collection of ovaries from the abattoir does not constitute animal research and is exempt from further review. Ovaries (~150 ovaries/collection) were placed immediately into PBS and then transported to the University of Kansas Medical Center at 20°C–24°C within 2.5–3 h. Follicular diameters were determined by individually measuring follicle diameters; follicles were designated into three different groups based on diameter (3–5 mm—small, 6–9 mm—medium and >9 mm—large). Follicular fluid was aspirated using a tuberculin syringe (28 gauge needle) for small follicles and a 5 ml syringe with a 20-gauge needle for medium and large follicles. Follicular fluid from individual follicles was then stored independently or pooled into 15 ml aliquots based on experimental designs.

Isolation of extracellular vesicles

Extracellular vesicles were isolated using a differential ultracentrifugation method developed for serum isolation of exosomes [17] and recently validated for FF [18]. Follicular fluid was diluted 1:1 with PBS and then spun at 800 g for 5 min to pellet all cells including oocytes (the cell pellets were snap-frozen at –80°C or placed in Trizol). Follicular fluid was then centrifuged at 2000 g for 20 min followed by 12,000 g for 45 min to remove cellular debris and other large particles (large microvesicles and apoptotic blebs). Samples were then filtered through a 0.22-μm pore filter (Millipore) to further remove vesicles greater than 220 nm. Ultracentrifugation of the 1:1 mix FF: PBS was performed at 110,000 g for 3 h. Above centrifuge steps were perform in an Optima L-100XP ultracentrifuge, using a swinging bucket SW32Ti rotor for large-scale collection (15 ml FF). The resulting EV pellets were then resuspended in 4 ml PBS and spun again for 1.5 h at 110,000 g in a TLA 100.4 fixed angle rotor. A final wash with 1 ml of PBS was then performed and spun at 110,000 g for 1.5 h using a TLA 55 fixed angle rotor. All centrifugations were performed at 4°C. The obtained pellets were resuspended in PBS for further analysis. When FF volumes were below 2 ml, the TLA110.4 rotor was used in place of SW32Ti until the last ultracentrifugation with TLA55 rotor.

In order to remove co-precipitated materials, EVs collected from the ultracentrifugation protocol described above were then subjected to a size exclusion column, and the purification was performed per manual (Izon, MA). Briefly, before using the qEV column, column performance was monitored by the timing the flow through of wash buffer completely through the column as per manufacturer

instructions. Dilute ultracentrifuged EV preparations in PBS (500 μl of 1mg of EV protein) were then loaded into the qEV column followed by addition of 500 μl washing buffer aliquots each time until finishing collection. Eluted fractions (F: 500 μl) were collected immediately after loading of EVs. Extracellular vesicles were shown to elute in F8-F10 in a pilot study, this was consistent with manufacturer recommendations. These three fractions were then concentrated by a subsequent ultracentrifugation (110,000 g for 30 min) and resuspended in PBS for subsequent studies. Columns were then extensively washed and stored in 20% ethanol, until next use at which time their performance was evaluated. Any decrease in flow rate the column was discarded.

Nanoparticle tracking analysis

To determine particle size and concentration, nanoparticle tracking analysis (NTA) was performed with a Nanosight LM10 instrument (Nanosight, Salisbury, UK) outfitted with a LM14C laser. Each EV preparation was sampled three times to generate three independent dilutions. These dilutions range from ~1:1000 to 1:10,000 for each sample (the dilution is determined empirically for each sample) and then each of the three dilutions is analyzed three times. The overall average of these three dilutions was used as the experimental result for each sample. From validation studies using dilution series, we determined that NTA is most accurate between particle concentrations in the range of 2×10^8/ml to 2×10^9/ml. Thus, samples were diluted to this level and absolute concentrations were then back calculated according to the dilution factor.

Transmission electron microscopy

Extracellular vesicles (10 mg/ml) were fixed overnight (2% glutaraldehyde and 0.1 M cacodylate buffer) and washed with 0.1 M sodium cacodylate buffer. A glow discharge treated carbon film 300 mesh grid was inverted and floated upside down on the drop containing fixed EVs (20 min). Each grid was rinsed seven times with filtered distilled water and then stained with 1% uranyl acetate. All samples are examined in a JEOL-JEM-1400 transmission electron microscope at an 80–100 kV with 15,000× magnification.

Western blot analysis

Extracellular vesicle samples (10 μg protein) were lysed in SDS sample buffer with 50 mM DTT, heated for 5 min at 95°C, and subjected to electrophoresis using 12% SDS-PAGE in running buffer at constant 120 V for 1.5 h. Proteins were then electrotransferred onto polyvinylidenedifluoride membranes, and the membranes were blocked with 5% (w/v) skim milk powder in Tris-buffered saline with 0.05% (v/v) Tween-20 (TTBS) for 1 h at RT. Membranes were then probed with primary anti-CD81, anti-Mcl1, anti-Akt, and anti-actin antibodies overnight at 4°C in TTBS (50 mM Tris, 150 mM NaCl, 0.05% Tween20) followed by incubation with the secondary anti-mouse IgG or anti-sheep goat antibodies for 1 h. Antibody sources, dilutions, and method of validation are in Supplementary Table S1. Membranes were washed three times in TTBS for 10 min after each incubation step and detected by enhanced chemiluminescence (GE Healthcare Bio-science, PA) as per the manufacturer's instructions. To ensure that similar levels of total proteins were loaded on to westerns, we stained the membranes with Swift Membrane Stain (G Biosciences, St Louis MO) as per the manual instructions.

Granulosa cell culture

Primary GCs isolated from small, medium, and large follicles were cultured in DMEM/F12 supplemented with 1000 IU/ml penicillin, 1000 μg/ml streptomycin, 2 μg/ml recombinant human insulin, 1.1 μg/ml human transferrin, 1 ng/ml sodium selenite, and 10% fetal bovine serum (Atlanta biologicals, GA). Fetal bovine serum was diluted with equal volume of DMEM/F12 and spun for 3 h at 110,000 g to remove vesicles in advance. Cells were cultured at 38.5°C supplemented with 6% CO_2. Plating densities and specifics to assay are described below.

Extracellular vesicles labeling and imaging

Extracellular vesicles were stained using the PKH67 Green Fluorescent Cell Linker Kit (Sigma Chemical Corp, St Louis, MO) as per the manual protocol and pelleted by ultracentrifugation following several washes in PBS before final resuspension in PBS. To test if there is any residual or precipitant dye with this protocol, a negative control was performed in parallel under same protocol but without EVs. For the negative control, the same volume of PBS was added to the centrifuged tube. Granulosa cells from small follicles were cultured as previously described and treated with an equal volume of labeled EVs or negative control solution in a chamber slide. Extracellular vesicle uptake was then observed under a Zeiss Pascal 510 confocal microscope.

Flow cytometry

Bovine GCs from small follicles were plated in 24-well dishes at 10^5 cells/well with/without the treatment of labeled EVs and PP2, Src kinase inhibitor. After treatment, GCs were washed with PBS once before detaching by trypsinization. Trypsin was neutralized by adding complete medium and cells were collected by centrifugation. For apoptosis assay, GCs were treated with 100 μg/ml EV from small follicle and then stained with propidium iodide staining in advance to analysis. The fluorescence level of cells was used to determine the level of EVs uptake under a BD LSR II (BD Biosciences), and data were analyzed with BD FACSDiva software (BD Biosciences). For imaging flow cytometry, samples were run on a Amnis ImageStream®^{X} Mark II Imaging Flow Cytometer and analyzed with IDEAS® Software (EMD Millipore, Darmstadt, Germany). In each of the cell and EV samples, 10,000 and 100,000 objects were collected, respectively.

BrdU incorporation assay and cell attachment assay

Bovine GCs from small follicles were cultured in 96-well culture dishes at 5×10^3 cells/well with or without EVs (see individual figure for concentration) collected from specific size follicles as indicated. Cell proliferation was measured 24 h later as BrdU incorporation according to the manufacturer's protocol (Roche). For inhibitor studies, GCs were cultured as described with addition of indicated kinase inhibitors, including PP2 for Src kinase, Ly294002 (Sigma-Aldrich) for PI3K kinase, SB203580 (LC laboratories) for p38 kinase, U0126 for MEK1/2, and SP600125 for JNK kinase. PP3, a nonactive PP2 analog was also used as a negative control in specific experiments. Dosage ranges (presented in figures) were determined in pilot experiments, based on ranges used in other cells types. Sources and catalog numbers for inhibitors are noted in Supplementary Table S1. For analyzing the effect of EVs on cell attachment, bovine GCs from small follicles were cultured with EVs from small, medium, or large follicles with controls with/without FBS. Cells were seeded at the density of 4×10^5 cells/ml simultaneously with indicated supplements into 96-well plates. Cells were then rinsed with PBS three times and fixed with 4% paraformaldehyde for 15 min. After washing with PBS, the fixed cells were stained with crystal violet (5 mg/ml in 2% ethanol) for 10 min. Following washing with water to

remove the residual dye, the plate was air-dried and then 2% SDS was used to dissolve crystal violet. The plate was read at absorbance 550 nm on a FlexStation 3 Multi-Mode Microplate Reader (Molecular Devices).

KAM-880 antibody microarray

Twenty-four hours after treatment, GCs with EV treatment (100 μg/ml EVs from small follicle) and nontreatment control were washed twice with cold PBS before adding 200 μl of lysis buffer (20 mM MOPS pH7.0, 2 mM EGTA, 5 mM EDTA, 30 mM sodium fluoride, 60 mM β-glycerophosphate, 20 mM sodium pyrophosphate, 1 mM sodium orthovanadate, 1% Triton X-100, 1 mM phenylmethylsulfonylfluoride, 3 mM benzamidine, 5 μM pepstatin A, 10 μM leupeptin, 1 mM dithiothreitol). Lysates were sonicated (Model Q800R, Active Motif, CA) with the following protocol: amplification 75%, pulse on 15 s, pulse off 45 s, temperature 3°C. Samples were then spun twice at 16,000 g for 30 min each at 4°C before submitting on dry ice to Kinexus Bioinformatics Corp. (Vancouver BC, Canada). The KAM-880 antibody microarray includes 518 pan-specific and 359 phospho-site specific antibodies. The background of this specific array was described by McGinnis et al. [19].

Ingenuity pathway analysis

MicroRNAs which are abundant in the large follicles (i.e. might be predicted to be inhibitory to cell proliferation) were identified from our small RNA-seq (GEO-GSE74879) study [18]. Their respective target genes were predicted through the use of Ingenuity® Pathway Analysis (IPA®, QIAGEN Redwood City, www.qiagen.com/ingenuity) and these predicted target genes were then compared to the differentially expressed proteins/translation modifications (kinase array results) following EV treatment. The overlapping miRNA target genes and the kinase array identified proteins were then subjected to ingenuity pathway analysis (IPA) in order to identify possible cell signaling pathways.

RNA preparation

Total RNA was isolated from GCs of individual follicles with Trizol (Invitrogen) according to the manufacturer's protocol. Briefly, GCs were disrupted in 1 ml of Trizol reagent and incubated for 15 min at room temperature following the addition of 200 μl of chloroform. Subsequently, the aqueous solution was mixed with 500 μl of isopropanol. To facilitate precipitation and visualization of RNA pellet, 1 μl glycogen (20 μg/μl) was added together with the RNA-isopropanol mixture solution and incubated at RT for 10 min and spun at 12,000 g for 15 min at 4°C. The pellet was washed with 500 μl of 75% ethanol followed by centrifugation at 12,000 g for 5 min at 4°C. The RNA pellet was dried at room temperature and dissolved in 15 μl of RNase-free water. The RNA solution was then stored at –80°C. The concentration of RNA was determined using Nanodrop spectrophotometer ND-1000 (Thermo Scientific, Wilmington, DE).

Quantitative RT-PCR

Total RNA was reverse-transcribed using SuperScriptTM II Reverse Transcriptase (Life Technologies) with random primer per manufacturer's instruction. Quantitative PCR was then performed with 1:5 dilution of cDNA on an Applied Biosystems HT7900 sequence detector. Primer sets for bovine *Timp1* (forward: CAG AAC CGC AGT GAG GAG TTT, reverse: GAT GTG CAG GTG CCC ATT C) and U6 (forward: CTC GCT TCG GCA GCA CA, reverse: AAC GCT TCA CGA ATT TGC GT) were designed using Primer Express 3.0 software (Applied Biosystems). Samples were run in triplicate, and the $\Delta\Delta$Ct method was used to calculate the relative expression between the samples after normalization with U6. The presence of a single dissociation curve confirmed the amplification of a single transcript and lack of primer dimers.

Statistical analysis

All of the quantitative experiments were repeated at least with three biological replicates and were analyzed by one-way ANOVA with Newman-Kuels multiple comparison test performed using GraphPad Prism version 5.00 for Windows, GraphPad Software, San Diego California USA, www.graphpad.com. $P < 0.05$ was considered statistically significant.

Results

Follicular fluid extracellular vesicle characterization

Follicular fluid EVs were characterized using a battery of molecular and visual methods. Western blot analysis for the EV marker, CD81, indicated that the amount of CD81 decreased as follicle size increased [equivalent protein loaded (10 μg)/lane; Supplementary Figure S1A]. Nanoparticle tracking analysis indicated a single peak of 100–150 nm diameter particles across the different sized follicles (Supplementary Figure S1B), and particles in FF from 3–5 mm follicles (hereafter called small follicles) were more concentrated than in FF from 6–9 mm and >9 mm follicles (hereafter called medium and large follicles, respectively). Electron microscopy of EVs negatively stained on grids indicated the presence of a typical cup shape morphology in all the samples indicating the existence of EVs, smaller material (10–20 nm) was prominently observed in the background (Supplementary Figure S1C).

Follicular stage-specific extracellular vesicles modulate granulosa cell proliferation

Treatment of GCs for 24 h with EVs (100 μg protein/ml) from small antral follicles induced a 3.4-fold increase in BrdU incorporation compared to the nontreated controls, while EVs from medium and large follicles only increased BrdU incorporation 2.3- and 1.6-fold, respectively (Figure 1A). The effect of small follicle EVs on BrdU incorporation was further strengthen by showing that the effect of EVs was concentration dependent (4, 20, 100 μg/ml; Figure 1B). Treatment with EVs from small follicles increased GC number by 2.03-fold and 2.11-fold as determined by cell counts using a hematocytometer in two independent experiments (n = 2). In order to eliminate other confounding aspects that might influence the cell proliferation assay, we examined cell attachment and cell apoptosis following exposure to EVs. After 30 min of simultaneously seeding of GCs and EVs, the number of GCs which attached on the plate were not different across treatment groups but were higher than control (Figure 1C). Additionally, we observed no differences in GC apoptosis after treatment with EVs for 24 h as determined by propidium iodide staining followed by flow cytometry (Figure 1D).

Granulosa cell proliferative activity was greatest in response to EVs isolated from small follicles. Because pools of FF from multiple small follicles contain a mix of atretic and nonatretic follicles, we further refined the experiment by collecting FF from large numbers (~100 follicles/each replicate) of individual small antral follicles. These follicles were then individually determined to be either nonatretic or atretic based on GC expression of tissue inhibitor of

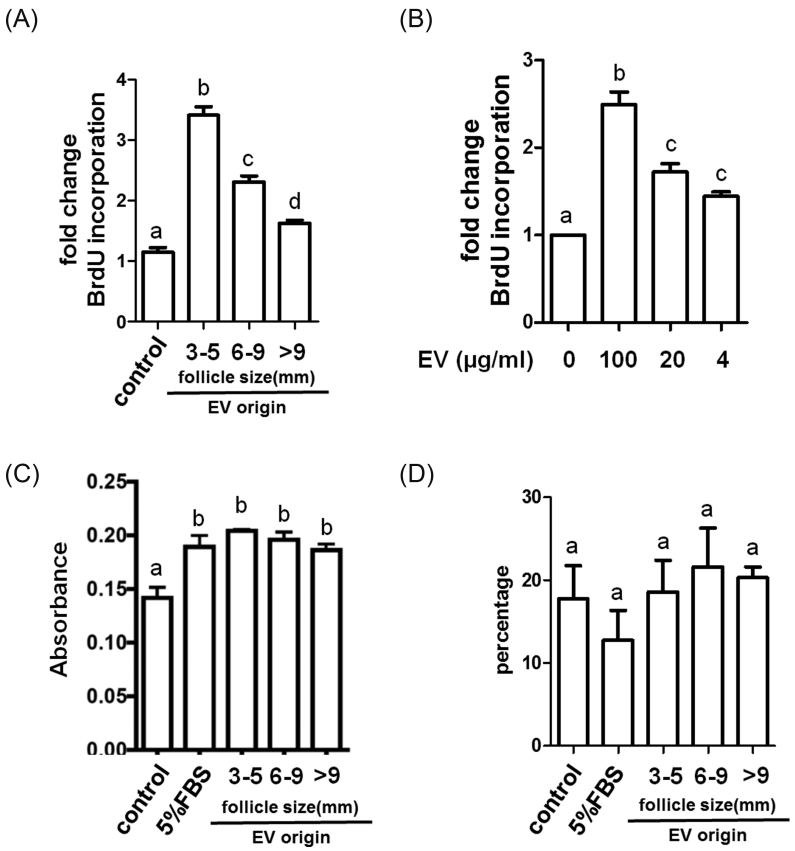

Figure 1. Effects of follicular fluid EVs on granulosa cell proliferation, attachment, and apoptosis. Granulosa cells were exposed to follicular fluid EVs from small (3–5 mm), medium (6–9 mm), and large (>9 mm) follicles and evaluated for effects on (A, B) cell proliferation, (C) cell attachment, and (D) apoptosis. Panel A depicts changes following 24 h exposure to EVs (100 μg/ml) from the different sized follicles. Panel B depicts a concentration-dependent effect of EVs from small antral follicles on cell proliferation. Panel C depicts effect of EVs from different sized follicles on cell attachment, while panel D depicts effect of EVs from different sized follicles on apoptosis. $^{a, b, c, d}$Means $\pm$ SEM (n = 3) with different superscripts were statistically different ($P < 0.05$).

metallopeptidase 1 (TIMP1) for each follicle [20]. Three independent collections were done to generate three pools of FF from atretic follicles and three pools from nonatretic follicles, and the EVs isolated from these pools were characterized for CD81 expression and the ability to influence cell proliferation. Follicular EVs from nonatretic and atretic follicles carried similar levels of EV marker CD81 and showed equivalent activities on GC proliferation (Supplementary Figure S2).

To further eliminate the possibility that residual molecules co-purifying with EVs (Supplementary Figure S1C) might be influencing cell proliferation, EVs were further purified through size exclusion columns. This purification step removed most of the residual molecules in the background yielding a highly purified preparation of follicular EVs (Figure 2A). This additional column purification step retained the GC proliferation activity (Figure 2B), and further indicates that the EVs are having a major influence on GC proliferation.

Extracellular vesicles from small follicles were preferentially taken up by granulosa cells

One explanation for the differential ability of EVs from small, medium, and large follicles to promote cell proliferation is that they may be taken up by the cells differentially. Granulosa cells were exposed to PKH67-fluorescently labeled EVs, confocal microscopy (optical sectioning) indicate that the green puncta observed in the EV exposed GCs reside within the cytosol of GCs indicating that EVs are taken up by GCs (Supplementary Figure S3B), little evidence of vesicular fusion can be seen with the plasma membrane of the GCs. Flow cytometry of GCs exposed to the fluorescently labeled EVs also indicated that the majority of cells uptake EVs (Supplementary Figure S3B). The potential effect of residual dye was excluded using a negative control (Supplementary Figure S3A).

To test if differential uptake may be occurring, EVs isolated from FF from different size follicles were labeled with PKH67 before treatment of GCs. Extracellular vesicles from small antral follicles exhibited a preferential uptake by GCs, irrespective of the source of GCs [i.e. small, medium (Supplementary Figure S4A), and large (Supplementary Figure S4B) antral follicles]. Therefore, for the rest of the experiments described here, GCs from small follicles are used. The intensity of green-positive cells as determined by flow cytometry following treatment with PKH67 labeled EVs from small follicles was twice that observed following treatment of EVs from medium and large antral follicles at both 2 and 24 h (Figure 3A). To further evaluate cellular uptake, another preparation of EVs from small follicles, which had half the numbers of EVs as determined by protein concentration were tested (particle concentration of FF-EV is proportional to its protein concentration, Supplementary Figure S5). Even with half the number of small follicle EVs, GC uptake was still greater for the small follicle-derived EVs versus those from medium and large follicles (Figure 3B). ImageStream imaging flow cytometry confirmed

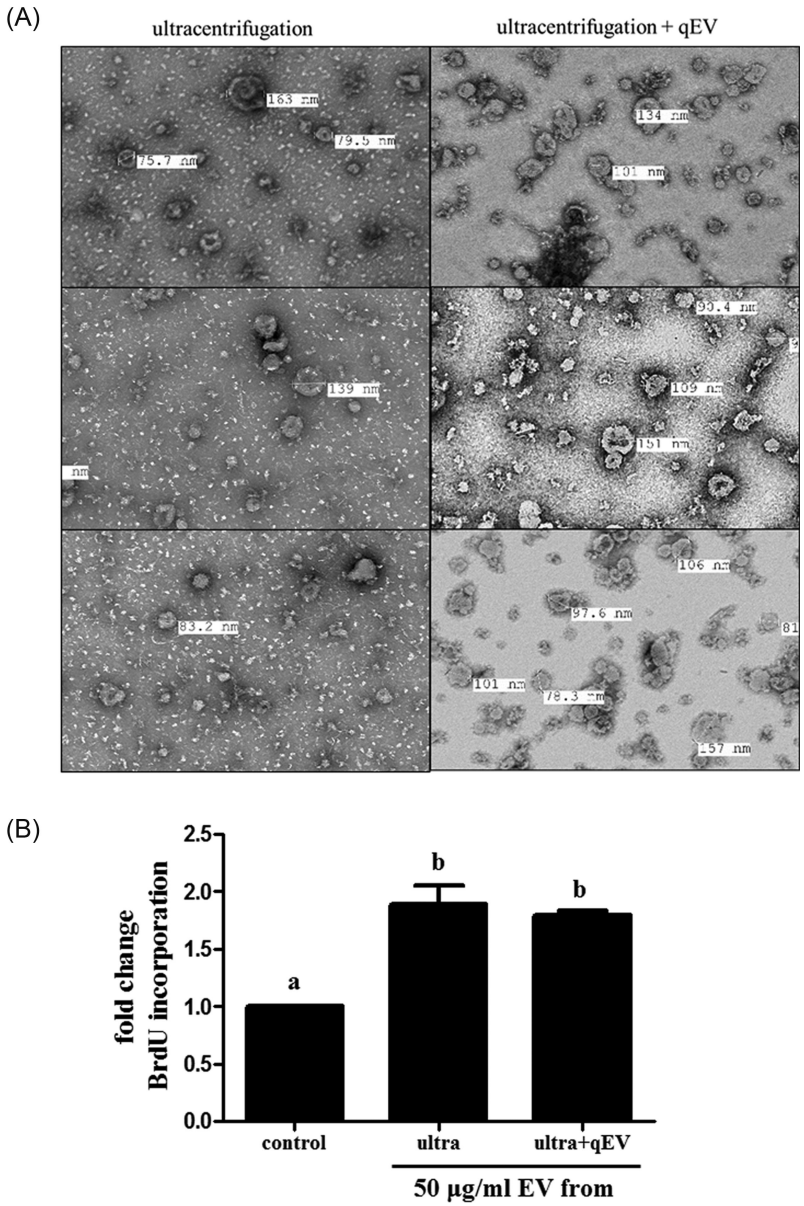

Figure 2. Comparison of the purity and activity of EV preparations following isolation by ultracentrifugation or ultracentrifugation plus size exclusion chromatography. Extracellular vesicles (from small follicles) isolated by both protocols were (A) imaged under TEM, and (B) activities on cell proliferation were tested. [a, b]Means ± SEM (n = 3) with different superscripts were statistically different ($P < 0.05$).

that GCs took up EVs isolated from small follicles at twice the level as EVs isolated from large follicles (Figure 3C), consistent with standard flow cytometry results in Figure 3A. The internalized EVs can be observed in the cells as green cytoplasmic puncta (Figure 3D). Amount of EVs loaded was based on protein concentration, but in addition to prove that a similar number of EVs were used, particle concentrations (numbers) of EVs from small and large follicles were quantified by NTA and Imagestream flow cytometry. Both these methods confirmed that similar concentrations of EVs from small and large follicles were used in these experiments (Figure 3E–G).

Small follicle extracellular vesicles affect granulosa cell protein kinase cell signaling

To examine the cell signaling pathways that mediate the actions of EVs on the GCs, we used a Kinexus antibody-based array that examines 877 cell signaling proteins. Bovine GCs from small follicles were treated with or without EVs (100 μg protein/ml) for 24 h as above and then cell lysates were collected and subjected to the antibody array. A total of 106 cell signaling proteins changed more than 25% after EV treatment in GCs, with 66 increasing and 40 decreasing in total protein levels. Post-translational modification of proteins (i.e. phosphorylation) also changed in GCs exposed to EV. Examining only those that changed 25% or more after EV treatment this cutoff was established in a previous study to provide validated results [19], we observed that 67 exhibited increased and 19 exhibited decreased phosphorylation (Table 1). Two of the top upregulated genes, Akt and mcl1, were verified by western blot (Supplementary Figure S6). Table 1 shows that treatment with EVs increased activity in the Src pathway with a marked elevation in phosphorylation of Src at Tyr418 (Table 1). Treatment with EVs increased activity in the

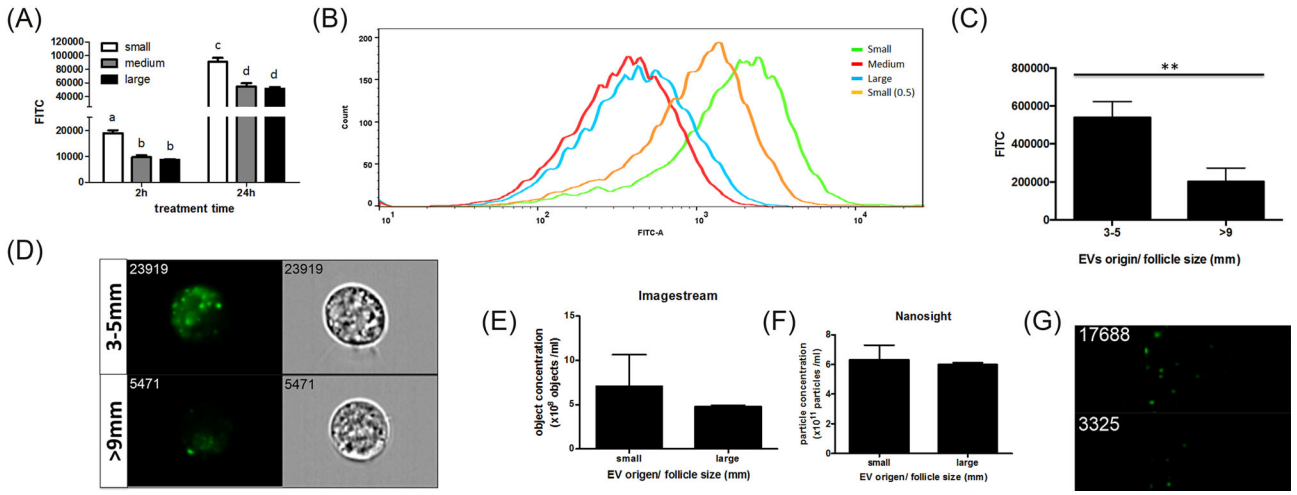

Figure 3. Extracellular vesicles from different sized antral follicles are differentially taken up by granulosa cells. Bovine granulosa cells from small antral follicles were cultured with PKH67-labeled EVs from small, medium, or large antral follicles for 2 or 24 h, and the level of uptake was measured by flow cytometry. (A) The level of EV uptake was determined by PKH67 intensity by flow cytometry. (B) Flow cytometry image showing the levels of uptake of PKH67-labeled EVs from different sized follicles including a set where EVs from small follicles were given at one half the dose (small 0.5). (C) Level of PKH67-labeled EV uptake was determined by PKH67 intensity under imageflow cytometry. (D) Representative images of GCs treated with PKH67-labeled EVs isolated from small and large follicles by imaging flow cytometry (ImageStream). Green PKH67 labeled EVs and corresponding light images of cells indicated internalization of EVs. (E) Equal EV loading was determined by imaging flow cytometry and (F) nanoparticle tracking analysis. (G) Images of labeled EVs (green spots) acquired by imaging flow cytometry are also shown. a,b,c,d and **Means ± SEM with different superscripts are different ($P < 0.05$).

PI3K/AKT pathway and its downstream molecules associated with cell growth (GSK3, mTOR, p70S6K) and survival (Mcl1 and NFκB). Treatment with EVs also elevated activity in the mitogen-activated protein kinase (MAPK) signaling pathway (Raf; MEKs 1, 2, 3/6, 5; ERKs 1, 3, 5; p38 MAPK; and RSK1). Elements of other signaling pathways were also observed in the data set (Ca^{2+}, PKC, JAK/STAT, Rac, etc.).

Analysis of cellular signaling pathways

In order to elucidate possible cell signaling pathways, we used a combined approach using kinase array data and miRNA expression data. Briefly, we examined those proteins/translational modifications, which were upregulated in response to EV treatment (from small follicles) and might be essential for EV-induced cell proliferation in small antral follicles. The genes associated with proliferation would be predicted to decline as small follicles become large follicles as cellular proliferation decreases during this transition. Since miRNA function primarily to suppress expression of their target transcripts, we evaluated whether abundant miRNA present in EVs from large follicles (compared to small follicles) from our previous study (GEO-GSE74879) [18] could modulate the expression of genes whose proteins were identified in the kinase array. We did this by comparing those predicted miRNA target genes to the list of proteins and phosphoproteins, which were increased in cells treated with EVs (Table 1). This analysis resulted in the identification of 101 genes that were subsequently analyzed by IPA. These 101 genes were highly related to post-translational modification, cell growth, proliferation, and survival and to the signaling pathways of HGF, Erbb, GnRH, and Src (Figure 4).

Src, PI3K, and MAPK signaling are implicated in extracellular vesicle-mediated cell proliferation

In order to test the IPA predictions and dissect out specific signaling pathways contributing to the EV-mediated cellular events, specific kinase inhibitors were applied into the cell culture system with/without the presence of EVs. Treatment with the Src inhibitor (PP2; 50 μM) completely blocked induction of cell proliferation (i.e. BrdU incorporation) by EV treatment while not affecting the proliferation of GCs receiving no treatment (Figure 5). To exclude the off-target effects, GCs were exposed to PP3 (a nonfunctional PP2 analog) in combination with EV treatment. PP3 did not influence EV-mediated cell proliferation at any concentration tested (Figure 5). To test the role of MAPKs in EV-mediated proliferation, GCs were treated with the MEK1/2 inhibitor (U0126; 0–50 μM), the JNK inhibitor (SP600125; 0–50 μM), or the p38 inhibitor (SB203580; 0–50 μM). Treatment with all concentrations of the JNK inhibitor effectively blocked EV-induced cell proliferation while not affecting the proliferation of cells receiving no treatment (Figure 5). Treatment of GCs with the p38 inhibitor reduced EV-induced proliferation at the highest concentration (Figure 5). Treatment with the MEK1/2 inhibitor decreased levels of EV-mediated proliferation with a dose-dependent trend but also affected the proliferation in the control groups (Figure 5). Treatment of GCs treated with the PI3K inhibitor LY294002; 0–50 μM) effectively blocked EV-induced cell proliferation and also reduced proliferation of cells receiving no treatment (Figure 5).

Src kinase was not required for uptake of extracellular vesicles

Src is known to regulate endocytosis which is one way for EVs to enter the cell [21]. To test if Src kinase activity affected the uptake of EVs by GCs, flow cytometry was used to define the level of uptake of PKH67-fluorescently labeled EVs following treatment with the Src kinase inhibitor, PP2 (Figure 6A). Treatment of PP2 did not influence uptake of EVs in GCs as the numbers of green-positive cells were similar despite increasing the concentration of the Src inhibitor (Figure 6A and B).

Table 1. Granulosa cell proteins showing a 25% increase or decrease upon EV treatment in the kinase array.

Name	Fold change	Name	Fold change	Name	Fold change	Name	Fold change
Src*	39.72	PP4C (X/C)*	1.46	p38g MAPK*	1.31	ASK1	0.71
Mcl1*	3.53	B-Raf	1.45	Histone H2A.X	1.30	Cdc25C	0.70
p53*	3.02	PKR1*	1.44	PKCe*	1.30	Rb	0.70
RSK1*	2.67	MEK2*	1.43	SMG1*	1.30	DUSP6	0.69
Akt1 (PKBa)*	2.59	Hsp90b	1.43	ERK5	1.30	Kit	0.69
GSK3a*	2.22	Csk*	1.43	ZIPK*	1.30	Cyclin D1	0.68
PKA R2a (PKR2)*	2.16	COX2*	1.43	Hsp70*	1.29	PDK1	0.68
MEK2*	2.10	Ezrin*	1.42	Bcr*	1.29	CD63	0.68
ERK3*	2.06	ALK*	1.42	Kit*	1.29	Krs-1	0.68
PKCh*	2.01	ERK1	1.42	Hpk1*	1.29	Myc	0.68
Ephrin-B2*	1.88	p21 CDKI1*	1.42	BRD2*	1.29	CDK6	0.68
Hsp27*	1.86	CDK2*	1.41	mTOR*	1.29	CDK4	0.67
Tau*	1.86	KDEL Receptor (KR10)*	1.41	I1PP2A (PHAPI)*	1.29	ErbB2	0.66
PI3K*	1.84	B23 (NPM)*	1.41	PAK1*	1.28	CDK9	0.66
NIK*	1.82	Cdc2 p34	1.41	hHR23B*	1.28	AMPKa2	0.66
BCL*	1.80	p53*	1.41	CaMK2a*	1.28	Synapsin 1	0.65
MEK3b	1.80	Rac1/cdc42*	1.40	MAPKAPK2*	1.28	Paxillin	0.65
Trail*	1.79	FAK*	1.40	MEK5	1.27	FAS	0.64
MEK1*	1.75	MEK1*	1.40	MEK2*	1.27	PAKa	0.64
eIF2a*	1.75	VIM*	1.39	PYKSD8	1.27	IRS1	0.64
CaMK1d*	1.74	VEGF-C*	1.38	MyoD*	1.27	WNK1	0.64
Chk1*	1.74	RIP2/RICK*	1.38	PTP1D/SHP2*	1.27	Fos	0.63
MEK3/6	1.70	ERK5*	1.38	MST3*	1.26	MEK1 + B23(NPM)	0.63
GNB2L1	1.69	Rac1	1.37	ErbB4*	1.26	STAT3	0.62
Nek2*	1.69	Akt1 (PKBa)*	1.37	PLCg1*	1.26	Bcl-xS/L	0.61
EGFR*	1.67	eIF4E*	1.37	Tau*	1.26	PTEN	0.60
c-Cbl*	1.66	B23 (NPM)*	1.37	PKCg*	1.26	STAT4	0.60
Caveolin 1*	1.64	PYK*	1.37	LIMK1/2*	1.26	NMDAR2B	0.59
Nek2*	1.62	Catenin a*	1.36	PKCd*	1.25	Src	0.57
PKCg*	1.61	ILK1*	1.36	ERK1	1.25	PKG1b-NT	0.56
ZAP70*	1.60	HDAC4/5/9*	1.36	JAK2*	1.25	PKCt	0.53
Fes*	1.59	MEK3*	1.35	Smad2*	1.25	JAK1	0.53
Hsp47*	1.58	PKCl*	1.35	Elk1*	1.25	HDAC4	0.51
FAK*	1.58	MLC*	1.35	MEKK2	0.75	Abl	0.50
MST3*	1.58	NFKB p65*	1.35	CD45	0.75	CDK2	0.50
Csk*	1.56	MST1*	1.34	STAT2	0.75	IRAK1	0.45
Hsp27*	1.54	Jun*	1.34	Chk1	0.75	Integrin a4	0.43
PKCt*	1.53	LAR*	1.34	PKA Ca/b	0.74	Hsc70	0.42
PKCm (PKD)*	1.52	Lck*	1.34	CDK5	0.74	VEGFR2	0.39
Crystallin aB	1.52	ERK1*	1.33	RONa	0.74	STAT1	0.35
NME7*	1.52	CAMK2d*	1.32	Progesterone receptor	0.74	STAT6	0.21
NFkappaB p65*	1.52	DNAPK	1.32	Rb	0.73	PKCl	0.05
CDK1*	1.51	SIK3*	1.32	Lck	0.73		
CPG16/CaMKinase VI*	1.51	Met*	1.32	JAK1	0.73		
FRK*	1.49	Cofilin*	1.31	GRK2	0.73		
TYK2	1.48	p70 S6K*	1.31	MEK3	0.73		
ANKRD3*	1.48	PKD (PKCm)*	1.31	IkBa	0.73		
CDK1/CDC2*	1.48	PP2A/Aa/b*	1.31	DUSP1 (MKP1)	0.72		
Caspase 3*	1.47	Cortactin*	1.31	MEK4	0.72		
HDAC5*	1.46	SOCS2*	1.31	Akt2 (PKBb)	0.71		

Shaded box: phosphorylated antibodies.

*Target of abundant miRNA in large antral follicle.

Discussion

This study provides the first evidence that EVs isolated from ovarian FF can stimulate GC proliferation in a stage-specific manner, and we have also shown that this differential activity of EVs in addition to the previously established differences in miRNA content and the presumed but unknown differences in protein and lipid contents may also be attributable to the differential capacity of EV uptake. This differential uptake seen for the small follicle-derived EVs provides a potential model for identification and studying of the presumed membrane proteins crucial for EV uptake. Additionally, we show that Src, MAPK, and PI3K pathways may mediate GC proliferation in response to EVs isolated from small follicles. Additionally, in this study we utilized a combination approach using the "gold" standard ultracentrifugation method combined with a column size exclusion

Top Canonical Pathways		
Name	p-value	Overlap
Molecular Mechanisms of Cancer	2.35E-36	9.6 % 35/365
HGF Signaling	2.91E-36	23.8 % 25/105
GNRH Signaling	8.56E-34	19.4 % 25/129
ErbB Signaling	1.06E-32	25.6 % 22/86
LPS-stimulated MAPK Signaling	1.87E-32	28.8 % 21/73

Top Upstream Regulators		
Upstream Regulator	p-value of overlap	Predicted Activation
nocodazole	6.45E-36	
TP53	1.58E-26	
ESR1	1.53E-21	
curcumin	1.36E-18	
SRC	2.28E-18	

Figure 4. Predicted downstream pathways involved in EV-mediated cellular proliferation. Targets of miRNA which are abundant in the large follicles (GEO-GSE74879) were predicted by IPA in advance and then compared to the genes which were regulated with the treatment of EVs from small follicles. The overlapping 101 genes were then subjected to IPA in order to predict the following regulator molecules and canonical signaling pathways in response to EV treatment.

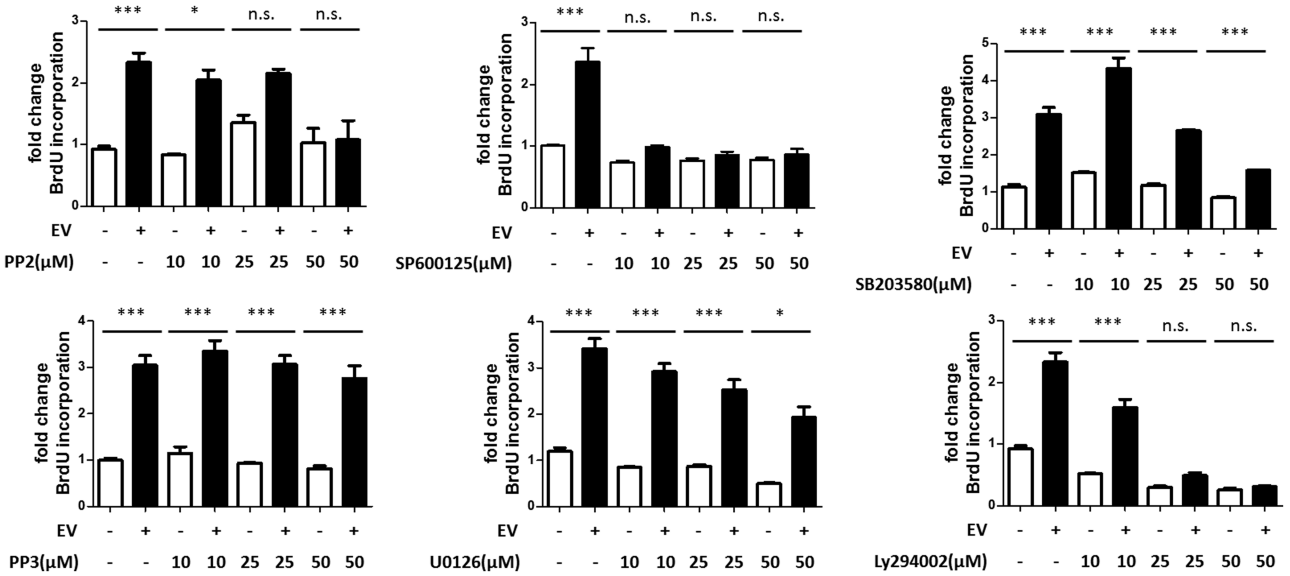

Figure 5. Testing of downstream signaling pathways affected by EV treatment. Specific inhibitors were used to elucidate downstream cell signaling pathways in granulosa cells following EV treatment. Pathways evaluated included Src (PP2), JNK (SP600125), PI3K (LY294002), MEK1/2 (U0126), and p38 (SB203580). A nonfunctional analog of PP2, PP3, was used to rule out potential off-target effects for the Src inhibition study. Means ± SEM (n = 3) were statistically different $^{*}(P < 0.05)$, $^{***}(P < 0.001)$.

method to significantly reduce/eliminate residual precipitants within the EV preparation.

Folliculogenesis is a well-orchestrated process regulated by endocrine, paracrine, and autocrine signaling [22]. Gonadotropins, which include follicle stimulating hormone (FSH) and luteinizing hormone (LH), are certainly the most critical and well-defined players serving as endocrine signaling hormones from the pituitary [23]. However, there are also paracrine and autocrine factors such as insulin-like growth factor, epidermal growth factor superfamily (Erb family, EGF ligands), hepatocyte growth factor (HGF), transforming growth factor beta superfamily, fibroblast growth factor, within the ovary, which have proven to be essential in stage-specific manners [24–26]. Extracellular vesicles isolated from FF of different physiological or pathological conditions have been reported to carry different miRNA, indicating a potential for being stage-specific signaling mediators [3–7, 12–14]. In this study, we showed that EVs isolated from FF of different size antral follicles exhibit differential activity on GC proliferation in which EVs from small follicles were most active. This differential activity of EVs was correlated to physiological condition where proliferation is highly active in small antral follicles. Surprisingly, no differences in the ability of GCs from different size follicles to respond to EVs were observed with respect to either cell proliferation or uptake. This could possibly be due to the inability of our current culture system to maintain and mimic the in vivo conditions seen in those physiologically different follicles.

The effects of EVs on cellular functions can be regulated through several manners including EV secretion, EV cargo selection, and EV

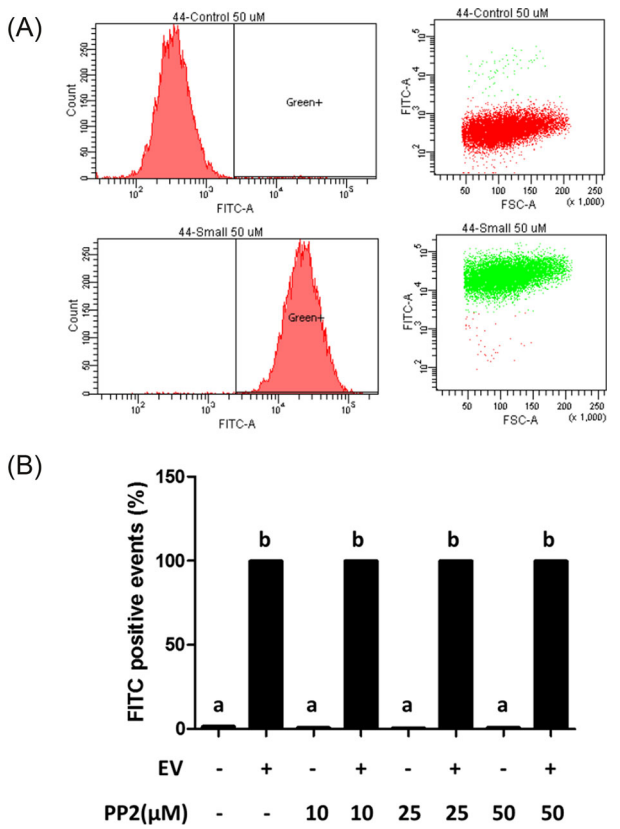

Figure 6. Effect of Src inhibition by PP2 on EV uptake. Influence of PP2 on EV uptake was tested by flow cytometry. (A) Representative image of effect of PP2 on EV uptake under flow cytometry (PP2: 50 μM), and (B) effect of PP2 on EV uptake in a dose-dependent design. ^{a,b}Means ± SEM with different superscripts were statistically different ($P < 0.05$).

uptake. Most studies on EV uptake focus on the ability of recipient cells to take up EVs [27]. Conventional and imaging flow cytometry were used to quantify the level of EV uptake after treatment of GCs with fluorescently labeled EVs, and both of them yielded very similar results. Three different approaches were used to ensure that the cells were given similar amounts of labeled EVs including determining protein concentration of EVs by the bicinchoninic acid assay, determining particle concentration by NTA and imaging flow cytometry. Extracellular vesicles were equally applied across treatment groups (small and large follicles) in the individual experiments based on these methods. Interestingly, NTA and imaging flow cytometry however yielded different absolute levels of EVs, and this can be attributed to methodological differences. Imaging flow cytometry relies on fluorescent labeling of EVs and subsequent detection; in contrast, NTA does not rely on fluorescence and individual particles are more likely to be counted. Based on our knowledge, this is the first demonstration showing that a single tissue (follicle) is able to produce stage-specific EVs, which have differential capacities of being taken up by specific target cells. This finding also enables follicular EVs as a potential model to identify surface proteins, which could be critical for EV uptake.

Granulosa cell proliferation is controlled by a complex signaling network [28]. Application of antibody-based array provided a comprehensive evaluation of EVs effects on signaling within recipient GCs. This analysis showed that active components of Src, PI3K/AKT, and MAPK signaling pathways were correlated with GC proliferation 24 h following stimulation with EVs. Combined with our previous small RNAseq on follicular EVs from different size follicles (GEO-GSE74879), we were able to identify several pathways (Src, HGF, GnRH, and ErbB pathways) that follicular EVs from small follicles may use to regulate GC proliferation. Indeed, the Src [29, 30], HGF [31], ErbB [32], and GnRH [33] pathways are known to activate the signaling molecules identified in antibody-based Kinome array. Inhibitor studies enabled us to dissect these predicted pathways, and to identify Src, PI3K, and MAPK signaling as important for EV-induced cell proliferation. Src kinase has been shown as downstream of several signaling pathways in the GCs, which include FSH, LH, growth differentiation factor 9/bone morphogenetic protein 15, protein kinase C (PKC), and progesterone [34–37]. Similarly, the PI3K and MAPK pathways have been reported to affect GC proliferation by regulating the cell cycle, and are associated with the actions of EGF and HGF [38, 39]. Here, we showed that follicular EVs can affect GCs through multiple cell signaling pathways. It is likely that the identified pathways intersect at crucial points to promote GC proliferation. The exact components of EVs that activate these pathways await discovery.

Isolation of follicular EVs began with a standard multistep ultracentrifugation protocol [17]. Differential ultracentrifugation is regarded as the best protocol to collect EVs from various body fluids because of its ability to pull down materials simply based on their density [40]. With a further step of sucrose gradient, we proved that the majority of vesicles collected by ultracentrifugation from FF contained the CD81 EV marker in our previous study [18]. However, the purity of postultracentrifugation EVs is still debated, and concern arises mainly because of the residual background materials observed under EM. To further eliminate and produce a highly purified EV preparation, we combined ultracentrifugation with a size exclusion column and successfully removed most of the small residual materials. The subsequent cell proliferation assays showed that the additional step of removing contaminating nonvesicle material did not influence the results of the BrdU incorporation assay, and thus strengthens the observation that EVs contributed most of the activity on inducing GC proliferation. Notwithstanding this further purification of the EVs, the effects of the EV treatment could be due to material within, on or tightly associated with the small follicle EVs. However, the fact that similar amounts of EVs from large follicles did not induce the same magnitude of cell proliferation as small follicle EVs provides evidence that the responses are due to the treatment and not to endogenous vesicles released by the cultured GCs. Our study provides an improved protocol for purifying EVs and provides strong evidence that EVs have the ability to alter GC physiology.

The bovine model for the study of reproduction is useful not only because of its importance to agriculture but also because it has many similarities to human reproduction; both species generate multiple follicular waves resulting in a single ovulation and the bovine reproductive cycle is nearly as long as the menstrual cycle of women. The availability of tissue and size of the bovine ovary makes it an effective model for studying the physiological role of follicular EVs and even the basic biology of EVs. When collecting EVs from the FF, one concern is the existence of atretic follicles. In our previous study, we proved that the majority of FF originating from 3–5 mm and >9 mm follicles was from nonatretic follicles [18]. In this study, we compared follicular EVs isolated from FF of nonatretic and atretic small follicles, which were separated based on expression of TIMP1,

a marker previously demonstrated to be increased in atretic follicles [20]. Surprisingly, follicular EVs from nonatretic and atretic small follicles exerted similar effects on the proliferation of GCs. This suggests that EVs isolated from small follicles inherently stimulate cell proliferation, and other factors control follicular atresia. This might suggest that the EVs isolated are highly similar and that the differences between these two types of follicles reside in the cell's ability to respond to the EVs. Further studies will be necessary to establish what differences/similarities exist in the atretic and nonatretic follicle EVs and/or whether cell responsiveness to EVs in these two types of follicles differ.

In conclusion, this study provides evidence that follicular EVs from different sized follicles exhibit different functional outcomes on GCs. Extracellular vesicles from highly proliferative small follicles were shown to induce GC proliferation while those from large antral follicles were only able to moderately stimulate proliferation. We also proved the activity is mainly from EVs and not residual materials that simultaneously co-precipitate with the EVs; therefore, these studies support the use of the ultracentrifugation EV collection methodology. The ability of EVs to induce cell proliferation was clearly prevented by inhibitors of the Src, PI3K, and MAPK signaling pathways. We also observed a differentially capacity of EVs being taken up by GCs. Interestingly, this difference in EV uptake was dependent upon the source of follicular EVs (i.e. small or large follicles), and was not dependent upon the size of the follicle from which the cells were isolated. Ultimately, the differential effects of EVs from different sized follicles could be due both a combination of differences in uptake and differences in content already established for miRNA, and presumed but unknown differences in proteins, lipids, etc. These studies support a role for EVs in modulating GC function within the developing antral follicles.

Supplementary data

Supplementary data are available at *BIOLRE* online.

Supplementary Figure S1. Characterization of follicular fluid EVs. Extracellular vesicles from small (3–5 mm), medium (6–9 mm), and large (>9 mm) antral follicles were subjected to (A) western blot analysis for the EV marker, CD81, using equal volumes of protein as demonstrated by a total protein staining, (B) nanoparticle tracking analysis (NTA) shows the mean size distribution and numbers of particles for three independent samples at the three follicle sizes and (C) transmission electron microscopy of negative stained EVs. Sizes of select individual EVs are shown in nanometers.

Supplementary Figure S2. Comparison of EVs from nonatretic and atretic follicles. (A) Follicles were categorized by expression of TIMP1 (delta Ct method) as nonatretic or atretic. For each replication (n), a three Ct difference was used to define the groups, FF from all follicles that exhibited an intermediate delta Ct were discarded. (B) The fold change in BrdU incorporation for the pooled follicular EVs from nonatretic (n = 3) or atretic (n = 3) follicles is shown. $^{a, b}$Means ± SEM with different superscripts were statistically different ($P < 0.05$).

Supplementary Figure S3. Uptake of fluorescently labeled EVs by bovine granulosa cells. Bovine granulosa cells from 3–5 mm follicles were exposed to PKH67-labeled EVs isolated from small bovine antral follicles and then subjected to confocal imaging (upper) and flow cytometry (lower). (A) Granulosa cells exposed to negative control showed no staining and complete lack of fluorescence by flow cytometry. (B) Treatment of granulosa cells with labeled EVs showed punctate staining after 24 h of incubation, and FITC intensity detected by flow cytometry was confirmed by confocal microscopy.

Supplementary Figure S4. Extracellular vesicles from different sized antral follicles are differentially taken up by granulosa cells of medium and large follicles. Bovine granulosa cells from (A) medium and (B) large antral follicles were cultured with labeled EVs from small, medium, or large antral follicles for 2 h, and the level of uptake was measured under flow cytometry.

Supplementary Figure S5. Particle concentration of follicular EVs is proportional to its protein concentration. Three independent collections of EVs were collected from FF. Their particle and protein concentrations were then determined and plotted into a histogram.

Supplementary Figure S6. Western blot validation of kinase array results. Western blot analysis for Mcl1 and Akt confirmed that these top Kinase array proteins were increased. Equal protein loading was observed as indicated by similar actin levels.

Supplementary Table S1. Antibody and inhibitor sources, antibody dilutions used, and validation methods.

Acknowledgments

We would like to thank Dr Randal Halfmann at the Stowers Institute for facilitating the ImageStream Analysis conducted in these experiments. We also thank Duane and Marlys Buenting for their assistance in transportation of the raw materials for this project.

Author Contributions

W-TH and LKC conceived and designed the study. W-TH performed experiments, W-TH and LKC analyzed the data and wrote the paper. PZ, JSD, TK, RN, and LKM contributed expertise and reagents. All authors edited and reviewed the manuscript.

References

1. Hennet ML, Combelles CM. The antral follicle: a microenvironment for oocyte differentiation. *Int J Dev Biol* 2012; **56**:819–831.
2. Rodgers RJ, Irving-Rodgers HF. Formation of the ovarian follicular antrum and follicular fluid. *Biol Reprod* 2010; **82**:1021–1029.
3. da Silveira JC, Veeramachaneni DN, Winger QA, Carnevale EM, Bouma GJ. Cell-secreted vesicles in equine ovarian follicular fluid contain miRNAs and proteins: a possible new form of cell communication within the ovarian follicle. *Biol Reprod* 2012; **86**:71.
4. Sohel MM, Hoelker M, Noferesti SS, Salilew-Wondim D, Tholen E, Looft C, Rings F, Uddin MJ, Spencer TE, Schellander K, Tesfaye D. Exosomal and non-exosomal transport of extra-cellular microRNAs in follicular fluid: implications for bovine oocyte developmental Competence. *PLoS One* 2013; **8**:e78505.
5. Santonocito M, Vento M, Guglielmino MR, Battaglia R, Wahlgren J, Ragusa M, Barbagallo D, Borzi P, Rizzari S, Maugeri M, Scollo P, Tatone C et al. Molecular characterization of exosomes and their microRNA cargo in human follicular fluid: bioinformatic analysis reveals that exosomal microRNAs control pathways involved in follicular maturation. *Fertil Steril* 2014; **102**:1751–1761 e1751.
6. Diez-Fraile A, Lammens T, Tilleman K, Witkowski W, Verhasselt B, De Sutter P Benoit Y, Espeel M, D'Herde K. Age-associated differential microRNA levels in human follicular fluid reveal pathways potentially determining fertility and success of in vitro fertilization. *Hum Fertil (Camb)* 2014; **17**:90–98.
7. Sang Q, Yao Z, Wang H, Feng R, Wang H, Zhao X, Xing Q, Jin L, He L, Wu L, Wang L. Identification of microRNAs in human follicular fluid: characterization of microRNAs that govern steroidogenesis in vitro and are associated with polycystic ovary syndrome in vivo. *J Clin Endocrinol Metab* 2013; **98**:3068–3079.

8. Cocucci E, Meldolesi J. Ectosomes and exosomes: shedding the confusion between extracellular vesicles. *Trends Cell Biol* 2015; **25**:364–372.
9. Kowal J, Tkach M, Thery C. Biogenesis and secretion of exosomes. *Curr Opin Cell Biol* 2014; **29**:116–125.
10. Alenquer M, Amorim MJ. Exosome biogenesis, regulation, and function in viral infection. *Viruses* 2015; **7**:5066–5083.
11. Cheung KH, Keerthikumar S, Roncaglia P, Subramanian SL, Roth ME, Samuel M, Anand S, Gangoda L, Gould S, Alexander R, Galas D, Gerstein MB et al. Extending gene ontology in the context of extracellular RNA and vesicle communication. *J Biomed Semantics* 2016; **7**:19.
12. Moreno JM, Nunez MJ, Quinonero A, Martinez S, de la Orden M, Simon C, Pellicer A, Diaz-Garcia C, Dominguez F. Follicular fluid and mural granulosa cells microRNA profiles vary in in vitro fertilization patients depending on their age and oocyte maturation stage. *Fertil Steril* 2015; **104**:1037–1046 e1031.
13. Roth LW, McCallie B, Alvero R, Schoolcraft WB, Minjarez D, Katz-Jaffe MG. Altered microRNA and gene expression in the follicular fluid of women with polycystic ovary syndrome. *J Assist Reprod Genet* 2014; **31**:355–362.
14. da Silveira JC, Winger QA, Bouma GJ, Carnevale EM. Effects of age on follicular fluid exosomal microRNAs and granulosa cell transforming growth factor-β signalling during follicle development in the mare. *Reprod Fertil Dev* 2015; **6**:897–905.
15. da Silveira JC, Carnevale EM, Winger QA, Bouma GJ. Regulation of ACVR1 and ID2 by cell-secreted exosomes during follicle maturation in the mare. *Reprod Biol Endocrinol* 2014; **12**:44.
16. Hung W, Christenson L, McGinnis L. Extracellular vesicles from bovine follicular fluid support cumulus expansion. *Biol Reprod* 2015; **93**(5):117.
17. Thery C, Amigorena S, Raposo G, Clayton A. Isolation and characterization of exosomes from cell culture supernatants and biological fluids. *Curr Protoc Cell Biol* 2006; 3:3.22.
18. Navakanitworakul R, Hung WT, Gunewardena S, Davis JS, Chotigeat W, Christenson LK. Characterization and small RNA content of extracellular vesicles in follicular fluid of developing bovine antral follicles. *Sci Rep* 2016; **6**:25486.
19. McGinnis LK, Pelech S, Kinsey WH. Post-ovulatory aging of oocytes disrupts kinase signaling pathways and lysosome biogenesis. *Mol Reprod Dev* 2014; **81**:928–945.
20. Hatzirodos N, Hummitzsch K, Irving-Rodgers HF, Harland ML, Morris SE, Rodgers RJ. Transcriptome profiling of granulosa cells from bovine ovarian follicles during atresia. *BMC Genomics* 2014; **15**: 40.
21. Donaldson JG, Porat-Shliom N, Cohen LA. Clathrin-independent endocytosis: a unique platform for cell signaling and PM remodeling. *Cell Signal* 2009; **21**:1–6.
22. Roy SK. Regulation of ovarian follicular development: a review of microscopic studies. *Microsc Res Tech* 1994; **27**:83–96.
23. Kumar TR. What have we learned about gonadotropin function from gonadotropin subunit and receptor knockout mice? *Reproduction* 2005; **130**:293–302.
24. Monget P, Bondy C. Importance of the IGF system in early folliculogenesis. *Mol Cell Endocrinol* 2000; **163**:89–93.
25. Knight PG, Glister C. TGF-beta superfamily members and ovarian follicle development. *Reproduction* 2006; **132**:191–206.
26. Chaves RN, de Matos MH, Buratini J, Jr, de Figueiredo JR. The fibroblast growth factor family: involvement in the regulation of folliculogenesis. *Reprod Fertil Dev* 2012; **24**:905–915.
27. Mulcahy LA, Pink RC, Carter DR. Routes and mechanisms of extracellular vesicle uptake. *J Extracell Vesicles* 2014; **3**:24641.
28. Field SL, Dasgupta T, Cummings M, Orsi NM. Cytokines in ovarian folliculogenesis, oocyte maturation and luteinisation. *Mol Reprod Dev* 2014; **81**:284–314.
29. Parsons SJ, Parsons JT. Src family kinases, key regulators of signal transduction. *Oncogene* 2004; **23**:7906–7909.
30. Thomas SM, Brugge JS. Cellular functions regulated by Src family kinases. *Annu Rev Cell Dev Biol* 1997; **13**:513–609.
31. Guglielmo MC, Ricci G, Catizone A, Barberi M, Galdieri M, Stefanini M, Canipari R. The effect of hepatocyte growth factor on the initial stages of mouse follicle development. *J Cell Physiol* 2011; **226**: 520–529.
32. Gavi S, Shumay E, Wang HY, Malbon CC. G-protein-coupled receptors and tyrosine kinases: crossroads in cell signaling and regulation. *Trends Endocrinol Metab* 2006; **17**:48–54.
33. Naor Z. Signaling by G-protein-coupled receptor (GPCR): studies on the GnRH receptor. *Front Neuroendocrinol* 2009; **30**:10–29.
34. Du XY, Huang J, Xu LQ, Tang DF, Wu L, Zhang LX, Pan XL, Chen WY, Zheng LP, Zheng YH. The proto-oncogene c-src is involved in primordial follicle activation through the PI3K, PKC and MAPK signaling pathways. *Reprod Biol Endocrinol* 2012; **10**:58.
35. Mottershead DG, Ritter LJ, Gilchrist RB. Signalling pathways mediating specific synergistic interactions between GDF9 and BMP15. *Mol Hum Reprod* 2012; **18**:121–128.
36. Rice VM, Chaudhery AR, Oluola O, Limback SD, Roby KF, Terranova PF. Herbimycin, a tyrosine kinase inhibitor with Src selectivity, reduces progesterone and estradiol secretion by human granulosa cells. *Endocrine* 2001; **15**:271–276.
37. Yamashita Y, Okamoto M, Ikeda M, Okamoto A, Sakai M, Gunji Y, Nishimura R, Hishinuma M, Shimada M. Protein kinase C (PKC) increases TACE/ADAM17 enzyme activity in porcine ovarian somatic cells, which is essential for granulosa cell luteinization and oocyte maturation. *Endocrinology* 2014; **155**:1080–1090.
38. Oktem O, Buyuk E, Oktay K. Preantral follicle growth is regulated by c-Jun-N-terminal kinase (JNK) pathway. *Reprod Sci* 2011; **18**:269–276.
39. Sriraman V, Modi SR, Bodenburg Y, Denner LA, Urban RJ. Identification of ERK and JNK as signaling mediators on protein kinase C activation in cultured granulosa cells. *Mol Cell Endocrinol* 2008; **294**: 52–60.
40. Szatanek R, Baran J, Siedlar M, Baj-Krzyworzeka M. Isolation of extracellular vesicles: Determining the correct approach (Review). *Int J Mol Med* 2015; **36**:11–17.